Energy Harvesting and Nonlinear Dynamics of a Two-Degree of Freedom Master-Slave System Integrated with a Piezoelectric Actuator

Mohamed Nagah, Wedad A. Elganini, Nasser. A. Saeed

***Abstract*—This study explores the dynamics of a piezoelectric energy harvester coupled with a master-slave system. The entire system is modeled as a two-degree-of-freedom system (2-DOF), along with a first-order differential equation governing the dynamics of the harvested voltage. The perturbation method is applied to derive the slow-flow modulating equations that govern the master-slave oscillation amplitudes and phases. By analyzing various response curves, the effects of different system parameters on both vibration amplitudes and harvesting voltage are investigated. The findings indicate that the system can be controlled as a vibration control or energy harvester. Optimal parameters for energy harvesting as well as for vibration control purposes are reported based on analytical investigations. The results are validated through numerical simulations with MATLAB algorithms (ODE45) using time response, phase plane, Poincaré map, and bifurcation diagram, where an excellent agreement between the numerical solutions and analytical investigations has been demonstrated.**

***Keywords*—Energy harvesting, stability, static bifurcation, vibration control, perturbation method, Poincaré-map.**

I. . INTRODUCTION

Recent advancements in remote monitoring and integrated circuit technology have led to a growing interest in self-powered wireless low-power electronic components. These devices can be powered by harnessing energy from the surrounding environment using vibration energy harvesting technology. Piezoelectric vibration energy harvesting technology offers several excitation types for collectors and different working modes, making it a promising approach to power such devices.

Manuscript received [07 September 2023]; accepted [17 December 2023]. Date of publication [17 January 2024].

Mohamed Nagah is with Faculty of Electronic Engineering , Department of Physics and Engineering Mathematics, , Menouf 32952, Menoufia University ,Egypt (email: mohamedzakinagah@gmail.com)

Wedad A. Elganini is with Faculty of Electronic Engineering , Department of Physics and Engineering Mathematics, , Menouf 32952, Menoufia University ,Egypt (email: wedad.elganaini@hotmail.com)

Nasser. A. Saeed is with Faculty of Electronic Engineering , Department of Physics and Engineering Mathematics, , Menouf 32952, Menoufia University ,Egypt. Department of Automation, Biomechanics, and Mechatronics, Faculty of Mechanical Engineering, Lodz University of Technology, 90924 Lodz, Poland (email: Nasser.a.Saeed@el-eng.menofia.edu.eg).

Despite the significant progress made in this area and extensive reviews, there are still several challenging issues to address, such as improving the efficiency of energy harvesting and addressing power management issues to ensure continuous operation, we added a piezoelectric , RC circuit and nonlinear stiffness between master and slave system In order to enhance the versatility of the system, efforts were made to expand its functionality beyond being solely a vibration controller, allowing it to also function as an energy harvester.

Future research directions in this field include developing novel materials with improved piezoelectric properties, designing more efficient energy harvesting systems, and developing advanced power management strategies to ensure reliable and continuous operation of such devices [1-3]. The addition of a nonlinear coupling spring element to the vibration absorber can improve its performance by offering more design flexibility, accommodating larger amplitude vibrations, and reducing resonant peaks in the system. It is worth noting, however, that nonlinearities in the system can cause dynamic instabilities, leading to an increase in vibration amplitudes instead of their reduction, which can facilitate more energy harvesting [4,5]. Combinational resonance can occur in a system due to its nonlinear behavior, where multiple frequencies interact nonlinearly, resulting in nearly periodic vibrations with significant amplitudes. Similarly, one-to-one internal resonance can arise when different vibration modes exhibit a specific mathematical relationship, causing nonlinear interaction and energy exchange. Both of these situations can cause dynamic instabilities and amplify vibration amplitudes, requiring careful system design and analysis to mitigate these challenges [6]. There has been a significant interest in using piezoelectric vibration-based energy harvesters as potential power sources for electronic devices, as indicated by several literature reviews on the subject [7]. New and improved techniques for harvesting energy using piezoelectric materials have been explored by scientists. However, the efficient vibration energy harvesting using these methods remains an ongoing area of research. In the past, the focus was mainly on increasing power density by targeting a single linear resonance frequency [8]. Although the performance of energy harvesters is generally limited to a narrow frequency range, it can be improved by utilizing a linear anti-resonance regime and optimizing the resistive load to achieve higher power output [9]. The primary aim of designing energy harvesting devices is to achieve resonance at multiple frequencies, resulting in increased efficiency and power output. To improve device efficiency,

researchers have proposed an L-shaped piezoelectric structure that can resonate at two frequencies. In addition to linear resonance, nonlinearity has also been explored by researchers to enhance the performance of energy harvesting systems. By selecting suitable parameters, researchers can achieve broadband energy harvesting by enhancing the electrical power harvested at various frequencies of ambient vibrations [10].

To broaden the operational frequency bandwidth for a given drive acceleration amplitude and increase power density, an alternative approach for vibration energy harvesting is to utilize parametric resonance. However, the presence of nonlinear attachments in the harvester can lead to hysteresis behavior in the frequency response near resonance [11]. For extracting energy across a wide frequency range, it is advisable to operate in the vicinity of quasi-periodic vibrations away from resonance. To achieve optimal energy efficiency in both single-degree-of-freedom (SDOF) and multi-degree-of-freedom (MDOF) mechanical systems, various techniques have been utilized [12]. Multi-degree-of-freedom (MDOF) systems have a wide range of applications in various fields, including industrial machinery [13-15], Vehicles used for transportation [16,17], Vibration induced by wind and human movement can be harnessed to generate energy. Dual-mass or multi-mass vibration energy harvesters have been shown to have superior energy harvesting capabilities compared to their single-mass counterparts [18]. Engineers have recently been concentrating on introducing nonlinearities in vibration absorbers or tuned mass damper systems to improve energy harvesting performance in engineering structures such as vehicle suspensions, tall buildings, and large flexible bridges. This technique is especially beneficial in dealing with random forces or motion excitations [19,20].

Numerous innovative designs for energy harvesting and vibration suppression (NES) have been suggested, and both experimental and analytical investigations have been conducted to explore these methods. One study investigated a new piezoelectric energy harvesting approach that utilized NES and demonstrated its ability to achieve a broad range of power output [21]. in a different study, integrated vibration suppression and piezoelectric energy harvesting were examined for a primary oscillator exposed to harmonic excitation. The study noted quasi-periodic responses near the resonance frequency, leading to decreased resonant amplitude, wider energy harvesting bandwidth, and targeted energy transfer [22, 23]. Two additional studies were centered on the utilization of piezoelectric materials for the suppression of mechanical vibration and energy harvesting [24, 25].

The effectiveness of a vibration absorber consisting of a simple mass-spring-damper system in suppressing nonlinear vibrations in a weakly nonlinear oscillator subjected to periodic external excitation was investigated in the first study, we compare our work with [24] Based on the findings, it was determined that adding a piezoelectric and nonlinear stiffness enhance the flexibility of the system to act not only as a vibration controller but also as an energy harvester.

. In the second study, a nonlinear energy sink (NES) absorber coupled to an electric circuit through a piezoelectric mechanism was explored for periodic and quasi-periodic vibration-based energy harvesting. Both studies utilized mathematical techniques to analyze the systems and showed the efficacy of the suggested solutions.

This paper investigates a two-degree-of-freedom system coupled with a first-order differential equation to harvest electrical voltage. The perturbation method is utilized to derive the slow-flow modulating equations governing the oscillation amplitudes. We examine how different system parameters affect the vibration amplitudes and harvesting voltage through response curves, showing that the system can display either periodic or quasi-periodic motion depending on these parameters. We conduct analytical investigations to determine the optimal system parameters for energy harvesting and vibration control purposes. Additionally, we conduct numerical simulations using various techniques and find that the results obtained numerically agree very well with the analytical findings.

II. I

I. MATHEMATICAL MODEL AND FREQUENCY-RESPONSE EQUATION

A. Mathematical model

The equations of motion that describe the nonlinear oscillations of the master-slave system coupled with a piezoelectric RC −circuit as shown in Figure (1), can be expressed as follows [31, 32]:

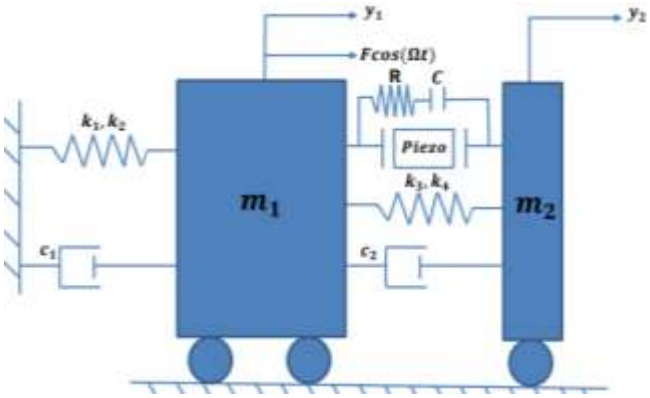

Figure 1: Two-degree-of-freedom mechanical system coupled to a piezoelectric RC −circuit.

$$m_1\ddot{y}_1 \quad c_1\dot{y}_1 \quad k_1y_1 + k_2y_1^3 + k_3(y_1 - y_2) + k_4(y_1 - y_2)^3 + c_2(\dot{y}_1 \quad \dot{y}_2) \quad {}_1y_3 = F\cos(\Omega t) \tag{1.a}$$

$$m_2\ddot{} \quad \dot{} \quad \dot{} \quad {}_2 - y_1) + k_4(y_2 - y_1)^3 = \eta_2 y_3 \tag{1.b}$$

$$\dot{} \quad \frac{1}{R} \quad \dot{} \quad \dot{} \tag{1.c}$$

where y_1, $\dot{y}_1$, and $\ddot{y}_1$ are the displacement, velocity, and acceleration of the master system, y_2, $\dot{y}_2$, and $\ddot{y}_2$ denote the displacement, velocity, and acceleration of the slave system, y_3 represents the harvesting voltage of piezoelectric

RC −circuit, m_1 and m_2 denote the master and slave masses, respectively, c_1 and c_2 are the linear damping coefficients of the master and slave systems, respectively. k_1 and k_2 are the linear and nonlinear damping coefficients of the master system, k_3 and k_4 are the linear and nonlinear damping coefficients of the slave system, F, and Ω denote the excitation force amplitude and its frequency, respectively. η_1 , η_2 and η_3 are the electro-mechanical coupling coefficients. c and R represent the electrical capacitance and resistance of the electrical circuit. By introducing the dimensionless parameters $x_1 = \frac{y_1}{h}$, $x_2 = \frac{y_2}{h}$, $v = \frac{y_3}{h}$, $\tau = \omega_n t$, and $\omega_n = \sqrt{\frac{k_1}{m_1}}$ (where h is a representative length) into Equations (1a)-(1c), one can obtain the following dimensionless equations of motion:

$$\ddot{X}_1 \quad {}_1\dot{X}_1 \quad {}_1^2X_1 \quad {}_1(X_1 \quad X_2) \quad {}_2(\dot{X}_1 \quad \dot{X}_2)$$
$$\alpha_1 x_1^3 + \alpha_2 (x_1 - x_2)^3 + \gamma_1 V = f\cos(\vartheta\tau) \tag{2.a}$$

$$\ddot{} \quad \dot{} \quad \dot{} \quad \dot{} \quad - \beta_3 x_1 + \alpha_3 (x_2 - x_1)^3 = \gamma_2 V \tag{2.b}$$

$$\dot{} \quad {}_3(\dot{} \quad \dot{} \tag{2.c}$$

where

$\Delta = \frac{m_1}{m_2}$, $\mu_1 = \frac{c_1}{\sqrt{(m_1 k_1)}}$, $\mu_2 = \frac{c_2}{\Delta\sqrt{(m_1 k_1)}}$, $\beta_1 = \frac{k_3}{k_1}$, $\beta_2 = \Delta\mu_2$, $\beta_3 = \frac{1}{\Delta}\beta_1$, $\alpha_1 = \frac{k_2 h^2}{k_1}$, $\alpha_2 = \frac{k_4 h^2}{k_1}$, $\alpha_3 = \frac{1}{\Delta}\alpha_2$, $\gamma_1 = \frac{\eta_1 v_0}{h k_1}$, $\gamma_2 = \frac{\gamma_1}{\Delta}$, $\gamma_3 = \frac{\eta_2 h}{c v_0}$, $f = \frac{F}{h k_1}$, $\vartheta = \frac{\Omega}{\omega_n}$, $\eta = \sqrt{\frac{m_1}{c^2 R^2 k_1}}$

B. Perturbation Analysis

To investigate the dynamical behaviors of the nonlinear system given by Equations (2a) - (2c), an approximate solution has been sought applying multiple time scales method as follows [26, 27]:

$$x_1(t,\varepsilon) = x_{11}(T_0,T_1) + \varepsilon x_{12}(T_0,T_1) + O(\varepsilon^2) \tag{3.a}$$

$$x_2(t,\varepsilon) = x_{21}(T_0,T_1) + \varepsilon x_{22}(T_0,T_1) + O(\varepsilon^2) \tag{3.b}$$

$$v(t,\varepsilon) = \varepsilon v_1(T_0,T_1) + \varepsilon^2 v_2(T_0,T_1) + O(\varepsilon^2) \tag{3.c}$$

where ε is the perturbation parameter, $T_0 = \tau$ and $T_1 = \varepsilon\tau$ are the fast and slow time scales of the system motion. In terms of T_0 and T_1, the ordinary derivatives $\frac{d}{d\tau}$ and $\frac{d^2}{d\tau^2}$ can be expressed as follows:

$$\frac{d}{dt} = D_0 + \varepsilon D_1, \quad \frac{d^2}{dt^2} = D_0^2 + 2\varepsilon D_0 D_1, \quad D_j = \frac{\partial}{\partial T_j}, \quad j = 0,1,2 \tag{4}$$

To make damping, nonlinearities, and primary resonance force appear in the same perturbation equations, we scale the equation parameters as follows:

$$\left.\begin{aligned} &\mu_1 = \varepsilon\hat{\mu}_1, \quad \mu_2 = \varepsilon\hat{\mu}_2, \quad \alpha_1 = \varepsilon\hat{\alpha}_1, \quad \alpha_2 = \varepsilon\hat{\alpha}_2, \\ &\alpha_3 = \varepsilon\hat{\alpha}_3, \quad \beta_1 = \varepsilon\hat{\beta}_1, \quad \beta_2 = \varepsilon\hat{\beta}_2, \quad \beta_3 = \varepsilon\hat{\beta}_3, \\ &f = \varepsilon\hat{f}, \quad \gamma_2 = \varepsilon\hat{\gamma}_2 \end{aligned}\right\} \tag{5}$$

Substituting Equations (3)-(5) into Equations (2a)-(2c) with equating the coefficients of the same power of ε, we have

$O(\varepsilon^0)$:

$$(D_0^2 + \omega_1^2)x_{11} = 0 \tag{6.a}$$

$$(D_0^2 + \omega_2^2)x_{21} = 0 \tag{6.b}$$

$O(\varepsilon^1)$:

$$\begin{aligned}(D_0^2 + \omega_1^2)x_{12} = &-2D_0D_1x_{11} - (\hat{\mu}_1 + \hat{\beta}_2)D_0x_{11} \\ &-\hat{\alpha}_1x_{11}^3 - \hat{\alpha}_2x_{11}^3 + \hat{\alpha}_2x_{21}^3 + 3\hat{\alpha}_2x_{11}^2x_{21} \\ &-3\hat{\alpha}_2x_{11}x_{21}^2 - \hat{\beta}_1x_{11} + \hat{\beta}_1x_{21} + \hat{\beta}_2D_0x_{21} \\ &-\gamma_1V_1 + \hat{f}\cos(\vartheta\tau)\end{aligned} \tag{7.a}$$

$$\begin{aligned}(D_0^2 + \omega_2^2)x_{22} = &-2D_0D_1x_{21} - \hat{\mu}_2D_0x_{21} + \hat{\mu}_2D_0x_{11} \\ &+\hat{\beta}_3x_{11} - \hat{\alpha}_3x_{21}^3 + \hat{\alpha}_3x_{11}^3 \\ &+3\hat{\alpha}_3x_{21}^2x_{11} - 3\hat{\alpha}_3x_{11}^2x_{21} + \gamma_2V_1\end{aligned} \tag{7.b}$$

$$(D_0 + \eta)V_1 = \hat{\gamma}_3D_0x_{11} - \hat{\gamma}_3D_0x_{21} \tag{7.c}$$

The solution of the homogeneous differential equation given by Equation (6) can be expressed as follows:

$$\begin{aligned}x_{11}(T_0,T_1) &= A(T_1)e^{i\omega_1T_0} + \overline{A}(T_1)e^{-i\omega_1T_0} \\ &= A(T_1)e^{i\omega_1T_0} + cc\end{aligned} \tag{8.a}$$

$$\begin{aligned}x_{21}(T_0,T_1) &= B(T_1)e^{i\omega_2T_0} + \overline{B}(T_1)e^{-i\omega_2T_0} \\ &= B(T_1)e^{i\omega_2T_0} + cc\end{aligned} \tag{8.b}$$

where cc denotes the complex conjugate of the preceding terms. The coefficients $A(T_1)$ and $B(T_1)$ are unknown coefficients in T_1 at this stage of the analysis. They will be determined by eliminating the secular and small-divisor terms at the next approximation order. Inserting Equations (8) into Equations (7c), we get

$$\begin{aligned}V_1(T_0,T_1) &= f_1e^{i\omega_1T_0} + \overline{f}_1e^{-i\omega_1T_0} - f_2e^{i\omega_2T_0} + \overline{f}_2e^{i\omega_2T_0} \\ &= f_1e^{i\omega_1T_0} - f_2e^{i\omega_2T_0} + cc\end{aligned} \tag{9}$$

Where

$f_1 = (\omega_1^2\hat{\gamma}_3A + i\eta\omega_1\hat{\gamma}_3A)/(\omega_1^2 + \eta^2)$,
$\overline{f}_1 = (\omega_1^2\hat{\gamma}_3\overline{A} - i\eta\omega_1\hat{\gamma}_3\overline{A})/(\omega_1^2 + \eta^2)$,
$f_2 = (\omega_2^2\hat{\gamma}_3B + i\eta\omega_2\hat{\gamma}_3B)/(\omega_2^2 + \eta^2)$,
$\overline{f}_2 = (-\omega_2^2\hat{\gamma}_3\overline{B} + i\eta\omega_2\hat{\gamma}_3\overline{B})/(\omega_2^2 + \eta^2)$

Inserting Equations (9) into Equations (7a) and (7b), we have

$$(D_0^2+\omega_1^2)x_{12} = (-2i\omega_1 D_1 A - i\omega_1(\hat{\mu}_1+\hat{\beta}_2)A - 3\hat{\alpha}_1 A^2\bar{A} - 3\hat{\alpha}_2 A^2\bar{A} - 6\hat{\alpha}_2 AB\bar{B} - \hat{\beta}_1 A - \gamma_1 f_1)e^{i\omega_1 T_0} + (3\hat{\alpha}_2 B^2\bar{B} + 6\hat{\alpha}_2 A\bar{A}B + \hat{\beta}_1 B + i\omega_2\hat{\beta}_2 B + \gamma_1 f_2)e^{i\omega_2 T_0} + 3\hat{\alpha}_2 A^2\bar{B}e^{i(2\omega_1-\omega_2)T_0} - 3\hat{\alpha}_2\bar{A}B^2 e^{i(2\omega_2-\omega_1)T_0} - \hat{\alpha}_1 A^3 e^{3i\omega_1 T_0} - \hat{\alpha}_2 A^3 e^{3i\omega_1 T_0} + \hat{\alpha}_2 B^3 e^{3i\omega_2 T_0} + 3\hat{\alpha}_2 A^2 B e^{i(2\omega_1+\omega_2)T_0} - 3\hat{\alpha}_2 AB^2 e^{i(2\omega_2+\omega_1)T_0} + \frac{\hat{f}}{2}e^{i\vartheta T_0} + \text{cc} \quad (10.a)$$

$$(D_0^2+\omega_2^2)x_{22} = (-2i\omega_2 D_1 B - i\hat{\mu}_2\omega_2 B - 3\hat{\alpha}_3 B^2\bar{B} - 6\hat{\alpha}_3 A\bar{A}B - \gamma_2 f_2)e^{i\omega_2 T_0} + (i\hat{\mu}_2\omega_1 A + 3\hat{\alpha}_3 A^2\bar{A} + \hat{\beta}_3 A + 6\hat{\alpha}_3 AB\bar{B} + \gamma_2 f_1)e^{i\omega_1 T_0} + 3\hat{\alpha}_3\bar{A}B^2 e^{i(2\omega_2-\omega_1)T_0} - 3\hat{\alpha}_3 A^2\bar{B}e^{i(2\omega_1-\omega_2)T_0} - \hat{\alpha}_3 B^3 e^{3i\omega_2 T_0} + \hat{\alpha}_3 A^3 e^{3i\omega_1 T_0} + 3\hat{\alpha}_3 AB^2 e^{i(2\omega_2+\omega_1)T_0} - 3\hat{\alpha}_3 A^2 B e^{i(2\omega_1+\omega_2)T_0} + cc \quad (10.b)$$

To investigate the system dynamics at the simultaneous primary-internal resonance conditions ($\vartheta \to \omega_1,\ \omega_2 \to \omega_1$), let us introduce the parameters σ_1 and σ_2 to describe the considered resonance conditions as follows:

$$\vartheta = \omega_1 + \sigma_1 = \omega_1 + \varepsilon\hat{\sigma}_1, \quad \omega_2 = \omega_1 + \sigma_2 = \omega_1 + \varepsilon\hat{\sigma}_2 \quad (11)$$

Substituting Equation (11) into Equations (10a) and (10b), we can obtain the following solvability conditions of Equations (10):

$$-2i\omega_1 D_1 A - i\omega_1(\hat{\mu}_1+\hat{\beta}_2)A - 3\hat{\alpha}_1 A^2\bar{A} - 3\hat{\alpha}_2 A^2\bar{A} - 6\hat{\alpha}_2 AB\bar{B} - \hat{\beta}_1 A - \gamma_1 f_1 + (3\hat{\alpha}_2 B^2\bar{B} + 6\hat{\alpha}_2 A\bar{A}B + \hat{\beta}_1 B + i\omega_2\hat{\beta}_2 B + \gamma_1 f_2)e^{i(\hat{\sigma}_2)T_1} + 3\hat{\alpha}_2 A^2\bar{B}e^{-i\hat{\sigma}_2 T_1} - 3\hat{\alpha}_2\bar{A}B^2 e^{2i\hat{\sigma}_2 T_1} + \frac{\hat{f}}{2}e^{i\hat{\sigma}_1 T_1} = 0 \quad (12.a)$$

$$-2i\omega_2 D_1 B - i\hat{\mu}_2\omega_2 B - 3\hat{\alpha}_3 B^2\bar{B} - 6\hat{\alpha}_3 A\bar{A}B - \gamma_2 f_2 + (i\hat{\mu}_2\omega_1 A + 3\hat{\alpha}_3 A^2\bar{A} + \hat{\beta}_3 A + 6\hat{\alpha}_3 AB\bar{B} + \gamma_2 f_1)e^{-i\hat{\sigma}_2 T_1} + 3\hat{\alpha}_3\bar{A}B^2 e^{i\hat{\sigma}_2 T_1} - 3\hat{\alpha}_3 A^2\bar{B}e^{-2i\hat{\sigma}_2 T_1} = 0 \quad (12.b)$$

To investigate Equations (12a) and (12b), let us express A and B in the polar forms as follows [26, 27]:

$$A = \frac{1}{2}\hat{a}_1 e^{i\delta_1} \Rightarrow D_1 A = \frac{1}{2}\hat{a}_1' e^{i\delta_1} + \frac{1}{2}i\hat{a}_1\delta_1' e^{i\delta_1}, \quad a_1 = \varepsilon\hat{a}_1, \quad (13.a)$$

$$B = \frac{1}{2}\hat{a}_2 e^{i\delta_2} \Rightarrow D_1 B = \frac{1}{2}\hat{a}_2' e^{i\delta_2} + \frac{1}{2}i\hat{a}_2\delta_2' e^{i\delta_2}, \quad a_2 = \varepsilon\hat{a}_2 \quad (13.b)$$

where a_1 and a_2 are the steady-state amplitudes of the instantaneous displacements of the coupling piezo system, while δ_1 and δ_2 are the phases of the two motions. Inserting Equation (13) into Equations (12), with separating the real and imaginary parts, yields:

$$\frac{da_1}{dT_1} = -\frac{1}{2}(\hat{\mu}_1+\hat{\beta}_2)a_1 - \frac{1}{2}\frac{\eta\gamma_1\hat{\gamma}_3}{(\omega_1^2+\eta^2)}a_1 - \frac{1}{\omega_1}(\frac{1}{2}\hat{\beta}_1 a_2 + \frac{3}{8}\hat{\alpha}_2 a_2^3 + \frac{3}{4}\hat{\alpha}_2 a_1^2 a_2 + \frac{1}{2}\frac{\omega_2^2\gamma_1\hat{\gamma}_3}{(\omega_2^2+\eta^2)}a_2)\sin(\varphi_2) + \frac{1}{\omega_1}(\frac{1}{2}\omega_2\hat{\beta}_2 a_2 + \frac{1}{2}\frac{\omega_2\gamma_1\hat{\gamma}_3\eta}{(\omega_2^2+\eta^2)}a_2)\cos(\varphi_2) + \frac{\hat{f}}{2\omega_1}\sin(\varphi_1) + \frac{3}{8\omega_1}\hat{\alpha}_2 a_1^2\ a_2\sin(\varphi_2) + \frac{3}{8\omega_1}\hat{\alpha}_2 a_1\ a_2^2\sin(2\varphi_2) \quad (14.a)$$

$$\frac{da_2}{dT_1} = -\frac{1}{2}\hat{\mu}_2 a_2 - \frac{1}{2}\frac{\gamma_2\hat{\gamma}_3\eta}{(\omega_2^2+\eta^2)}a_2 + \frac{1}{\omega_2}(\frac{1}{2}\hat{\beta}_3 a_1 + \frac{3}{8}\hat{\alpha}_3 a_1^3 + \frac{3}{4}\hat{\alpha}_3 a_1 a_2^2 + \frac{1}{2}\frac{\omega_1^2\gamma_2\hat{\gamma}_3}{(\omega_1^2+\eta^2)}a_1)\sin(\varphi_2) + \frac{1}{\omega_2}(\frac{1}{2}\hat{\mu}_2\omega_1 a_1 + \frac{1}{2}\frac{\eta\omega_1\gamma_2\hat{\gamma}_3}{(\omega_1^2+\eta^2)}a_1)\cos(\varphi_2) - \frac{3}{8\omega_2}\hat{\alpha}_3 a_1 a_2^2\sin(\varphi_2) - \frac{3}{8\omega_2}\hat{\alpha}_3 a_1^2 a_2\sin(2\varphi_2) \quad (14.b)$$

$$\frac{d\varphi_1}{dT_1} = \hat{\sigma}_1 - \frac{3}{8\omega_1}\hat{\alpha}_1 a_1^2 - \frac{3}{8\omega_1}\hat{\alpha}_2 a_1^2 - \frac{3}{4\omega_1}\hat{\alpha}_2 a_2^2 - \frac{1}{2\omega_1}\hat{\beta}_1 - \frac{1}{2}\frac{\omega_1\gamma_1\hat{\gamma}_3}{(\omega_1^2+\eta^2)} + \frac{1}{\omega_1 a_1}(\frac{1}{2}\hat{\beta}_1 a_2 + \frac{3}{8}\hat{\alpha}_2 a_2^3 + \frac{3}{4}\hat{\alpha}_2 a_1^2 a_2 + \frac{1}{2}\frac{\omega_2^2\gamma_1\hat{\gamma}_3}{(\omega_2^2+\eta^2)}a_2)\cos(\varphi_2) + \frac{1}{\omega_1 a_1}(\frac{1}{2}\omega_2\hat{\beta}_2 a_2 + \frac{1}{2}\frac{\omega_2\gamma_1\hat{\gamma}_3\eta}{(\omega_2^2+\eta^2)}a_2)\sin(\varphi_2) + \frac{\hat{f}}{2\omega_1 a_1}\cos(\varphi_1) + \frac{3}{8\omega_1 a_1}\hat{\alpha}_2 a_1^2 a_2\cos(\varphi_2) - \frac{3}{8\omega_1 a_1}\hat{\alpha}_2 a_1 a_2^2\cos(2\varphi_2) \quad (14.c)$$

$$\frac{d\varphi_2}{dT_1} = -\hat{\sigma}_2 - (-\frac{3}{8\omega_1}\hat{\alpha}_1 a_1^2 - \frac{3}{8\omega_1}\hat{\alpha}_2 a_1^2 - \frac{3}{4\omega_1}\hat{\alpha}_2 a_2^2 - \frac{1}{2\omega_1}\hat{\beta}_1 - \frac{1}{2}\frac{\omega_1\gamma_1\hat{\gamma}_3}{(\omega_1^2+\eta^2)} + \frac{1}{\omega_1 a_1}(\frac{1}{2}\hat{\beta}_1 a_2 + \frac{3}{8}\hat{\alpha}_2 a_2^3 + \frac{3}{4}\hat{\alpha}_2 a_1^2 a + {}_2 + \frac{1}{2}\frac{\omega_2^2\gamma_1\hat{\gamma}_3}{(\omega_2^2+\eta^2)}a_2)\cos(\varphi_2) + \frac{1}{\omega_1 a_1}(\frac{1}{2}\omega_2\hat{\beta}_2 a_2 + \frac{1}{2}\frac{\omega_2\gamma_1\hat{\gamma}_3\eta}{(\omega_2^2+\eta^2)}a_2)\sin(\varphi_2) + \frac{\hat{f}}{2\omega_1 a_1}\cos(\varphi_1) + \frac{3}{8\omega_1 a_1}\hat{\alpha}_2 a_1^2 a_2\cos(\varphi_2) - \frac{3}{8\omega_1 a_1}\hat{\alpha}_2 a_1 a_2^2\cos(2\varphi_2)) - \frac{3}{8\omega_2}\hat{\alpha}_3 a_2^2 - \frac{3}{4\omega_2}\hat{\alpha}_3 a_1^2 - \frac{1}{2}\frac{\omega_2\gamma_2\hat{\gamma}_3}{(\omega_2^2+\eta^2)} + \frac{1}{\omega_2 a_2}(\frac{1}{2}\hat{\beta}_3 a_1 + \frac{3}{8}\hat{\alpha}_3 a_1^3 + \frac{3}{4}\hat{\alpha}_3 a_1 a_2^2 + \frac{1}{2}\frac{\omega_1^2\gamma_2\hat{\gamma}_3}{(\omega_1^2+\eta^2)}a_1)\cos(\varphi_2) - \frac{1}{\omega_2 a_2}(\frac{1}{2}\hat{\mu}_2\omega_1 a_1 + \frac{1}{2}\frac{\eta\omega_1\gamma_2\hat{\gamma}_3}{(\omega_1^2+\eta^2)}a_1)\sin(\varphi_2) + \frac{3}{8\omega_2 a_2}\hat{\alpha}_3 a_1 a_2^2\cos(\varphi_2) - \frac{3}{8\omega_2 a_2}\hat{\alpha}_3 a_1^2 a_2\cos(2\varphi_2) \quad (14.d)$$

where $\varphi_1 = \hat{\sigma}_1 T_1 - \delta_1$, $\varphi_2 = \delta_1 - \delta_2 - \hat{\sigma}_2 T_1$. Restoring the original parameters into Equation (14) (i.e., $\hat{\mu}_1 = \frac{\mu_1}{\varepsilon}, \hat{\mu}_2 = \frac{\mu_2}{\varepsilon}$, $\hat{\alpha}_1 = \frac{\alpha_1}{\varepsilon}, \hat{\alpha}_2 = \frac{\alpha_2}{\varepsilon}$, $\hat{\alpha}_3 = \frac{\alpha_3}{\varepsilon}$, $\hat{\beta}_1 = \frac{\beta_1}{\varepsilon}$, $\hat{\beta}_2 = \frac{\beta_2}{\varepsilon}$, $\hat{\beta}_3 = \frac{\beta_3}{\varepsilon}$, $\hat{\gamma}_2 = \frac{\gamma_2}{\varepsilon}$, and $\tau = \frac{T_1}{\varepsilon}$), we have

$$\frac{da_1}{d\tau} = -\frac{1}{2}(\mu_1+\beta_2)a_1 - \frac{1}{2}\frac{\eta\gamma_1\gamma_3}{(\omega_1^2+\eta^2)}a_1 - \frac{1}{\omega_1}(\frac{1}{2}\beta_1 a_2 + \frac{3}{8}\alpha_2 a_2^3 + \frac{3}{4}\alpha_2 a_1^2 a_2 + \frac{1}{2}\frac{\omega_2^2\gamma_1\gamma_3}{(\omega_2^2+\eta^2)}a_2)\sin(\varphi_2) + \frac{1}{\omega_1}(\frac{1}{2}\omega_2\beta_2 a_2 + \frac{1}{2}\frac{\omega_2\gamma_1\gamma_3\eta}{(\omega_2^2+\eta^2)}a_2)\cos(\varphi_2) + \frac{f}{2\omega_1}\sin(\varphi_1) + \frac{3}{8\omega_1}\alpha_2 a_1^2 a_2\sin(\varphi_2) + \frac{3}{8\omega_1}\alpha_2 a_1 a_2^2\sin(2\varphi_2) \quad (15.a)$$

$$\frac{da_2}{d\tau} = -\frac{1}{2}\mu_2 a_2 - \frac{1}{2}\frac{\gamma_2\gamma_3\eta}{(\omega_2^2+\eta^2)}a_2 + \frac{1}{\omega_2}(\frac{1}{2}\beta_3 a_1 + \frac{3}{8}\alpha_3 a_1^3 + \frac{3}{4}\alpha_3 a_1 a_2^2 + \frac{1}{2}\frac{\omega_1^2\gamma_2\gamma_3}{(\omega_1^2+\eta^2)}a_1)\sin(\varphi_2) + \frac{1}{\omega_2}(\frac{1}{2}\mu_2\omega_1 a_1 + \frac{1}{2}\frac{\eta\omega_1\gamma_2\gamma_3}{(\omega_1^2+\eta^2)}a_1)\cos(\varphi_2) - \frac{3}{8\omega_2}\alpha_3 a_1 a_2^2\sin(\varphi_2) - \frac{3}{8\omega_2}\alpha_3 a_1^2 a_2\sin(2\varphi_2) \quad (15.b)$$

$$\frac{d\varphi_1}{d\tau} = \sigma_1 - \frac{3}{8\omega_1}\alpha_1 a_1^2 - \frac{3}{8\omega_1}\alpha_2 a_1^2 - \frac{3}{4\omega_1}\alpha_2 a_2^2 - \frac{1}{2\omega_1}\beta_1 - \frac{1}{2}\frac{\omega_1\gamma_1\gamma_3}{(\omega_1^2+\eta^2)} + \frac{1}{\omega_1 a_1}(\frac{1}{2}\beta_1 a_2 + \frac{3}{8}\alpha_2 a_2^3 + \frac{3}{4}\alpha_2 a_1^2 a_2 + \frac{1}{2}\frac{\omega_2^2\gamma_1\gamma_3}{(\omega_2^2+\eta^2)}a_2)\cos(\varphi_2) + \frac{1}{\omega_1 a_1}(\frac{1}{2}\omega_2\beta_2 a_2 + \frac{1}{2}\frac{\omega_2\gamma_1\gamma_3\eta}{(\omega_2^2+\eta^2)}a_2)\sin(\varphi_2) + \frac{f}{2\omega_1 a_1}\cos(\varphi_1) + \frac{3}{8\omega_1}\hat{\alpha}_2 a_1 a_2\cos(\varphi_2) - \frac{3}{8\omega_1}\hat{\alpha}_2 a_2^2\cos(2\varphi_2) \quad (15.c)$$

$$\frac{d\varphi_2}{d\tau} = -\sigma_2 - (-\frac{3}{8\omega_1}\alpha_1 a_1^2 - \frac{3}{8\omega_1}\alpha_2 a_1^2 - \frac{3}{4\omega_1}\alpha_2 a_2^2 - \frac{1}{2\omega_1}\beta_1 - \frac{1}{2}\frac{\omega_1\gamma_1\gamma_3}{(\omega_1^2+\eta^2)} + \frac{1}{\omega_1 a_1}(\frac{1}{2}\beta_1 a_2 + \frac{3}{8}\alpha_2 a_2^3 + \frac{3}{4}\alpha_2 a_1^2 a_2 + \frac{1}{2}\frac{\omega_2^2\gamma_1\gamma_3}{(\omega_2^2+\eta^2)}a_2)\cos(\varphi_2) + \frac{1}{\omega_1 a_1}(\frac{1}{2}\omega_2\beta_2 a_2 + \frac{1}{2}\frac{\omega_2\gamma_1\gamma_3\eta}{(\omega_2^2+\eta^2)}a_2)\sin(\varphi_2) + \frac{f}{2\omega_1 a_1}\cos(\varphi_1) + \frac{3}{8\omega_1}\alpha_2 a_1 a_2\cos(\varphi_2) - \frac{3}{8\omega_1}\alpha_2 a_2^2\cos(2\varphi_2)) - \frac{3}{8\omega_2}\alpha_3 a_2^2 - \frac{3}{4\omega_2}\alpha_3 a_1^2 - \frac{1}{2}\frac{\omega_2\gamma_2\gamma_3}{(\omega_2^2+\eta^2)} + \frac{1}{\omega_2 a_2}(\frac{1}{2}\beta_3 a_1 + \frac{3}{8}\alpha_3 a_1^3 + \frac{3}{4}\alpha_3 a_1 a_2^2 + \frac{1}{2}\frac{\omega_1^2\gamma_2\gamma_3}{(\omega_1^2+\eta^2)}a_1)\cos(\varphi_2) - \frac{1}{\omega_2 a_2}(\frac{1}{2}\mu_2\omega_1 a_1 + \frac{1}{2}\frac{\eta\omega_1\gamma_2\gamma_3}{(\omega_1^2+\eta^2)}a_1)\sin(\varphi_2) + \frac{3}{8\omega_2}\alpha_3 a_1 a_2\cos(\varphi_2) - \frac{3}{8\omega_2}\alpha_3 a_1^2\cos(2\varphi_2) \quad (15.d)$$

Now, by substituting Equations (8), (9), (11), and (13) into Equation (3), we have.

$$x_1(\tau) = a_1(\tau)\cos\left(\vartheta\tau - \varphi_1(\tau)\right)$$

(16.a)

$$x_2(\tau) = a_2(\tau)\cos\left(\vartheta\tau - \varphi_1(\tau) + \varphi_2(\tau)\right)$$

(16.b)

The coupled master-slave-harvester system can be analyzed by solving Equation (15). Accordingly, at the steady-state oscillation of the master-slave system, we have $\frac{da_1}{d\tau} = \frac{da_2}{d\tau} = \frac{d\varphi_1}{d\tau} = \frac{d\varphi_2}{d\tau} = 0$. Setting this condition into Equations (15) yields the flowing nonlinear algebraic system:

$$F_1(a_1,a_2,\varphi_1,\varphi_2) = -\frac{1}{2}(\mu_1+\beta_2)a_1 - \frac{1}{2}\frac{\eta\gamma_1\gamma_3}{(\omega_1^2+\eta^2)}a_1 - \frac{1}{\omega_1}(\frac{1}{2}\beta_1 a_2 + \frac{3}{8}\alpha_2 a_2^3 + \frac{3}{4}\alpha_2 a_1^2 a_2 + \frac{1}{2}\frac{\omega_2^2\gamma_1\gamma_3}{(\omega_2^2+\eta^2)}a_2)\sin(\varphi_2) + \frac{1}{\omega_1}(\frac{1}{2}\omega_2\beta_2 a_2 + \frac{1}{2}\frac{\omega_2\gamma_1\gamma_3\eta}{(\omega_2^2+\eta^2)}a_2)\cos(\varphi_2) + \frac{f}{2\omega_1}\sin(\varphi_1) + \frac{3}{8\omega_1}\alpha_2 a_1^2\ a_2\sin(\varphi_2) + \frac{3}{8\omega_1}\alpha_2 a_1 a_2^2\sin(2\varphi_2) = 0 \quad (17.a)$$

$$F_2(a_1,a_2,\varphi_1,\varphi_2) = -\frac{1}{2}\mu_2 a_2 - \frac{1}{2}\frac{\gamma_2\gamma_3\eta}{(\omega_2^2+\eta^2)}a_2 + \frac{1}{\omega_2}(\frac{1}{2}\beta_3 a_1 + \frac{3}{8}\alpha_3 a_1^3 + \frac{3}{4}\alpha_3 a_1 a_2^2 + \frac{1}{2}\frac{\omega_1^2\gamma_2\gamma_3}{(\omega_1^2+\eta^2)}a_1)\sin(\varphi_2) + \frac{1}{\omega_2}(\frac{1}{2}\mu_2\omega_1 a_1 + \frac{1}{2}\frac{\eta\omega_1\gamma_2\gamma_3}{(\omega_1^2+\eta^2)}a_1)\cos(\varphi_2) - \frac{3}{8\omega_2}\alpha_3 a_1 a_2^2\sin(\varphi_2) - \frac{3}{8\omega_2}\alpha_3 a_1^2 a_2\sin(2\varphi_2) = 0 \quad (17.b)$$

$$F_3(a_1,a_2,\varphi_1,\varphi_2)=\sigma_1-\frac{3}{8\omega_1}\alpha_1a_1^2-\frac{3}{8\omega_1}\alpha_2a_1^2$$
$$-\frac{3}{4\omega_1}\alpha_2a_2^2-\frac{1}{2\omega_1}\beta_1-\frac{1}{2}\frac{\omega_1\gamma_1\gamma_3}{(\omega_1^2+\eta^2)}$$
$$+\frac{1}{\omega_1 a_1}(\frac{1}{2}\beta_1a_2+\frac{3}{8}\alpha_2a_2^3+\frac{3}{4}\alpha_2a_1^2a_2$$
$$+\frac{1}{2}\frac{\omega_2^2\gamma_1\gamma_3}{(\omega_2^2+\eta^2)}a_2)\cos(\varphi_2)$$
$$+\frac{1}{\omega_1 a_1}(\frac{1}{2}\omega_2\beta_2a_2+\frac{1}{2}\frac{\omega_2\gamma_1\gamma_3\eta}{(\omega_2^2+\eta^2)}a_2)\sin(\varphi_2)$$
$$+\frac{f}{2\,\omega_1 a_1}\cos(\varphi_1)+\frac{3}{8\omega_1}\alpha_2 a_1\, a_2\cos(\varphi_2)$$
$$-\frac{3}{8\omega_1}\alpha_2a_2^2\cos(2\varphi_2)$$
$$=0 \qquad (17.c)$$

$$F_4(a_1,a_2,\varphi_1,\varphi_2)=-\sigma_2-(-\frac{3}{8\omega_1}\alpha_1a_1^2-\frac{3}{8\omega_1}\alpha_2a_1^2$$
$$-\frac{3}{4\omega_1}\alpha_2a_2^2-\frac{1}{2\omega_1}\beta_1-\frac{1}{2}\frac{\omega_1\gamma_1\gamma_3}{(\omega_1^2+\eta^2)}$$
$$+\frac{1}{\omega_1 a_1}(\frac{1}{2}\beta_1a_2+\frac{3}{8}\alpha_2a_2^3+\frac{3}{4}\alpha_2a_1^2a_2$$
$$+\frac{1}{2}\frac{\omega_2^2\gamma_1\gamma_3}{(\omega_2^2+\eta^2)}a_2)\cos(\varphi_2)$$
$$+\frac{1}{\omega_1 a_1}(\frac{1}{2}\omega_2\beta_2a_2+\frac{1}{2}\frac{\omega_2\gamma_1\gamma_3\eta}{(\omega_2^2+\eta^2)}a_2)\sin(\varphi_2)$$
$$+\frac{f}{2\,\omega_1 a_1}\cos(\varphi_1)+\frac{3}{8\omega_1}\alpha_2a_1\, a_2\cos(\varphi_2)$$
$$-\frac{3}{8\omega_1}\alpha_2a_2^2\cos(2\varphi_2))-\frac{3}{8\omega_2}\alpha_3a_2^2$$
$$-\frac{3}{4\omega_2}\alpha_3a_1^2-\frac{1}{2}\frac{\omega_2\gamma_2\gamma_3}{(\omega_2^2+\eta^2)}+\frac{1}{\omega_2 a_2}(\frac{1}{2}\beta_3a_1$$
$$+\frac{3}{8}\alpha_3a_1^3+\frac{3}{4}\alpha_3a_1a_2^2+\frac{1}{2}\frac{\omega_1^2\gamma_2\gamma_3}{(\omega_1^2+\eta^2)}a_1)\cos(\varphi_2)$$
$$-\frac{1}{\omega_2 a_2}(\frac{1}{2}\mu_2\omega_1a_1+\frac{1}{2}\frac{\eta\omega_1\gamma_2\gamma_3}{(\omega_1^2+\eta^2)}a_1)\sin(\varphi_2)$$
$$+\frac{3}{8\omega_2}\alpha_3a_1a_2\cos(\varphi_2)-\frac{3}{8\omega_2}\alpha_3a_1^2\cos(2\varphi_2)$$
$$=0 \qquad (17.d)$$

By solving the above nonlinear equations in terms of the system parameter, one can obtain the bifurcation diagrams given in the following section. In addition, to investigate the stability of Equation (17) stability, let the solution of Equation (17) be $(a_{10}, a_{20}, \varphi_1, \varphi_2)$ and suppose $(a_{11}, a_{21}, \varphi_{11}, \varphi_{21})$ denote small perturbations, so one can express the following:

$$a_1=a_{10}+a_{11},\quad a_2=a_{20}+a_{21},\quad \varphi_1=\varphi_{10}+\varphi_{11},$$
$$\varphi_2=\varphi_{20}+\varphi_{21} \qquad (18)$$

According to Equation (18), we have

$$\frac{da_1}{d\tau}=\frac{da_{11}}{d\tau},\quad \frac{da_2}{d\tau}=\frac{da_{21}}{d\tau},\quad \frac{d\varphi_1}{d\tau}=\frac{d\varphi_{11}}{d\tau},$$
$$\frac{d\varphi_2}{d\tau}=\frac{d\varphi_{21}}{d\tau} \qquad (19)$$

Substituting Equations (18) and (19) into Equation (15), one can obtain the following linearized model:

$$\begin{bmatrix}\frac{da_{11}}{d\tau}\\ \frac{da_{21}}{d\tau}\\ \frac{d\varphi_{11}}{d\tau}\\ \frac{d\varphi_{21}}{d\tau}\end{bmatrix}=\begin{bmatrix}\frac{\partial F_1}{\partial a_{11}} & \frac{\partial F_1}{\partial a_{21}} & \frac{\partial F_1}{\partial \varphi_{11}} & \frac{\partial F_1}{\partial \varphi_{21}}\\ \frac{\partial F_2}{\partial a_{11}} & \frac{\partial F_2}{\partial a_{21}} & \frac{\partial F_2}{\partial \varphi_{11}} & \frac{\partial F_2}{\partial \varphi_{21}}\\ \frac{\partial F_3}{\partial a_{11}} & \frac{\partial F_3}{\partial a_{21}} & \frac{\partial F_3}{\partial \varphi_{11}} & \frac{\partial F_3}{\partial \varphi_{21}}\\ \frac{\partial F_4}{\partial a_{11}} & \frac{\partial F_4}{\partial a_{21}} & \frac{\partial F_4}{\partial \varphi_{11}} & \frac{\partial F_4}{\partial \varphi_{21}}\end{bmatrix}\begin{bmatrix}a_{11}\\ a_{21}\\ \varphi_{11}\\ \varphi_{21}\end{bmatrix} \qquad (20)$$

The coefficients of the above Jacobian matrix are given in the appendix. Accordingly, to investigate the stability of the nonlinear system given by Equation (15) can be explored by checking the eigenvalues of the linear system given by Equation (20) [28].

III. RESULTS AND DISCUSSIONS

A. Results

Given the obtained solution of Equation of motion (2) as given in Equation (16), designing the slave characteristics to function as a vibration absorber or energy harvester requires deep investigations for the system dynamics. The introduced analyses are obtained following the dimensionless system parameters:

$\Delta=0.12,\ f=0.2,\ \sigma_1=0,=0,\ \mu_1=0.008,\ \mu_2=0.006,$
$\beta_1=0.12,\ \beta_2=\Delta\mu_2,\ \beta_3=\frac{1}{\Delta}\beta_1,\ \alpha_1=0.36,\ \alpha_2=$
$0.009,\ \alpha_3=\frac{1}{\Delta}\alpha_2,\ \eta=1,\ \gamma_1=0.2,\ \gamma_2=\frac{\gamma_1}{\Delta},\ \gamma_3=0.2,$
and $\omega_1=\omega_2=1$, unless otherwise stated. Figure (2) illustrates the response curve of the master-slave system at three different values of the excitation force amplitudes f. The figure shows that the oscillation of the master system is

directly proportional to the excitation amplitudes. It is clear from the figure also that the harvester response curve is a difference between the master response curves and the slave response curves because piezoelectric material lies between the master and the slave. The effect of the parameter Δ on the system response curve is investigated through three different values of Δ (i.e., $\Delta = 0.12, 0.06,$ and 0.025) as illustrated in Figure (3). By examining Figure (3), one can deduce that increasing Δ from 0.025 to 0.12 shifts the response curve to the right making the master and harvester minimum vibration amplitude occur at $\sigma_1 \approx -0.3$, while decreasing Δ from 0.06 to 0.025 shifts the response curve to the left to a minimum oscillation of both the master and harvester system occurring at $\sigma_1 \approx 0.4$. Accordingly, by altering the mass ratio of the master and slave $\Delta = \frac{m_2}{m_1}$, depending on the desired purpose of the presented system to function as an absorber or energy harvester, one can obtain the lowest oscillation amplitude of the master system or the maximum harvesting voltage.

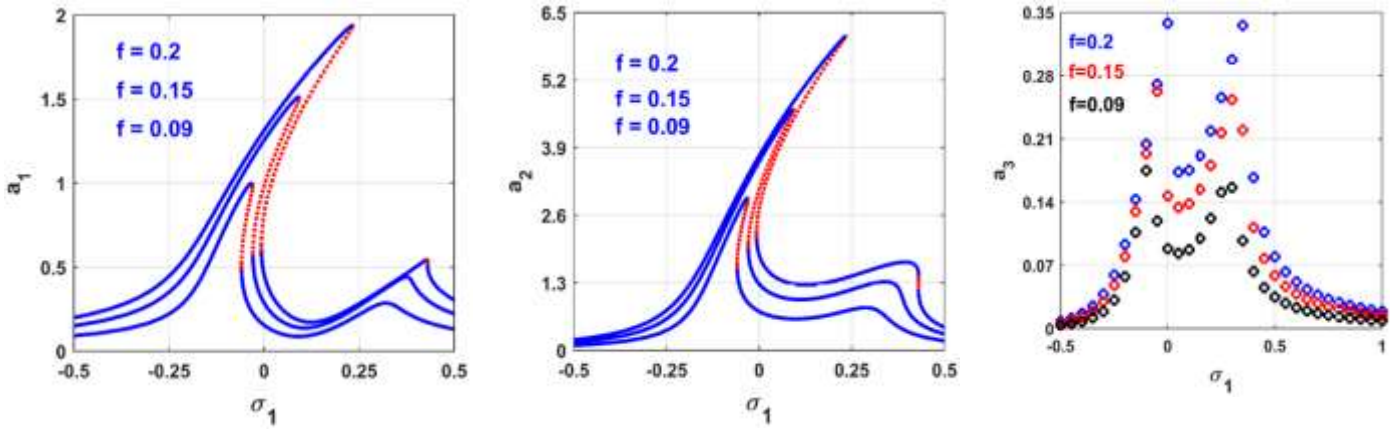

(a) (b) (c)

Figure 2. Oscillation amplitudes of the master-slave-harvester system at three different values of excitation $f = 0.2, 0.15,$ and 0.09: (a) master, (b) slave, and (c) harvester.

Based on Figure (3) when $\sigma_1 = 0.0$, the system's instantaneous oscillation and harvesting voltage are illustrated as shown in Figure (4) at three distinct master-slave mass ratio values Δ (i.e., when $\Delta = 0.025, 0.06,$ and 0.12). it is clear from the figure that the master system oscillates with a very small amplitude at $\Delta = 0.025$, while the slave system exhibits the maximum vibration amplitude at $\Delta = 0.12$. In this case (i.e., $\Delta = 0.12$), To prevent or lessen the nonlinear oscillation of the master system, the slave system acts as an absorber, absorbing all surplus energy brought on by the excitation force $f = 0.2$. However, the same figure demonstrates that the increase of the mass ratio from $\Delta = 0.025$ to $\Delta = 0.12$ maximizes the master oscillation amplitude by using the slave system as an exciter, which also raises the harvesting voltages. therefore, the presented system can be employed to operate as an absorber or energy-harvesting device by controlling the mass ratio. The effect of the master-slave linear stiffness ratio $\beta_1 = \frac{k_3}{k_1}$ on the system response curve has been illustrated in Figure (5). It is clear from the figure that β_1 acts like the mass ratio coefficient Δ, but increasing β_1 from 0.09 to 0.3 shifts the response curve to the right, while decreasing β_1 from 0.3 to 0.09 shifts the response curve to the left.

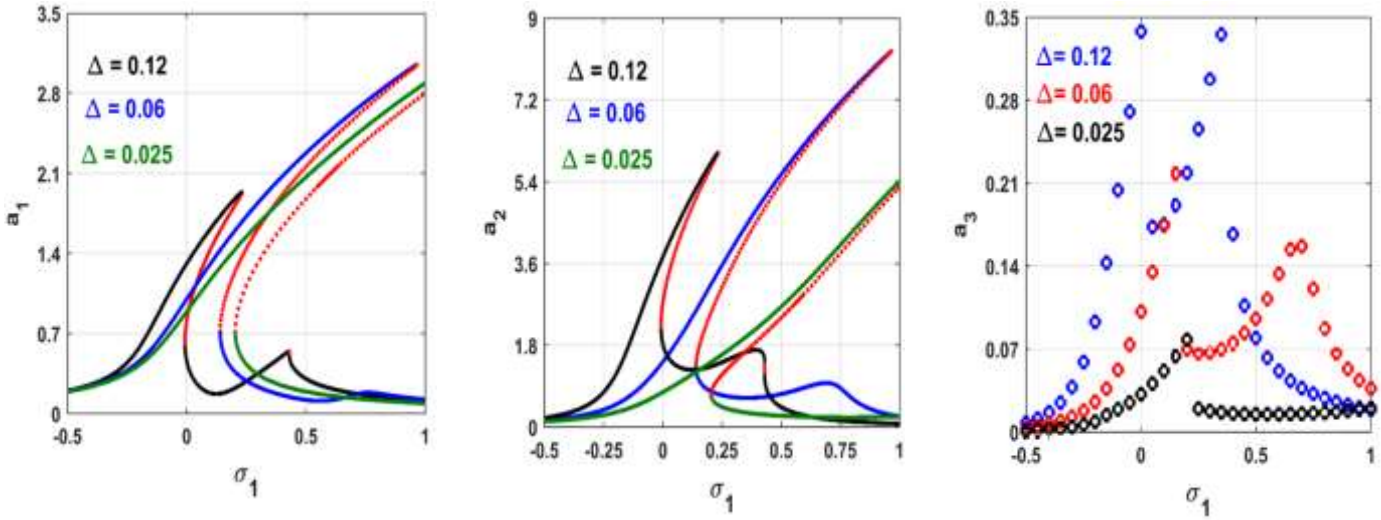

(a) (b) (c)

Figure 3. Oscillation amplitudes of the master-slave-harvester system at three different values of the master-slave mass ration $\Delta = \frac{m_2}{m_1} = 0.12, 0.06,$ and 0.025: (a) master, (b) slave, and (c) harvester.

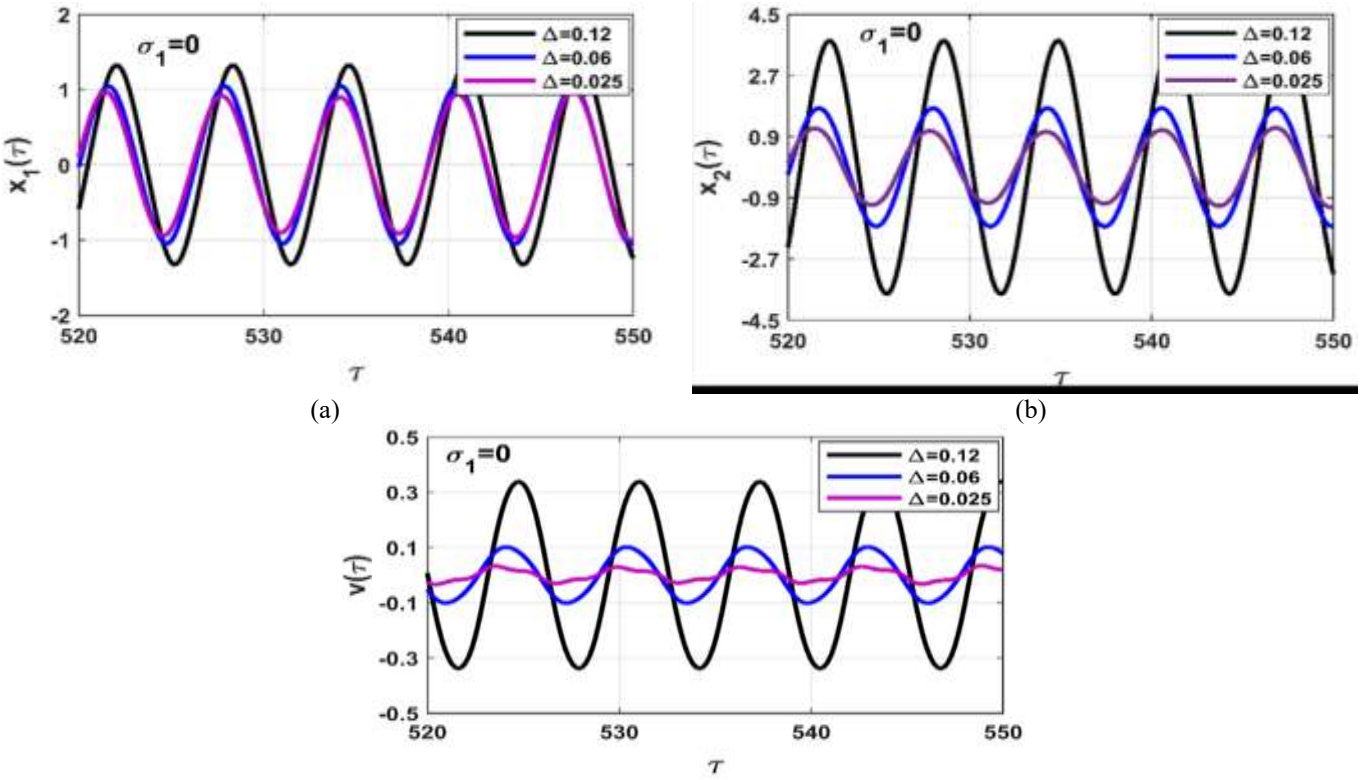

Figure 4. Time response of the master-slave-harvester system at three different values of the master-slave mass ratio $\Delta = \frac{m_2}{m_1} = 0.12, 0.06, and\ 0.025$ when $\sigma_1 = 0.0$: (a) master, (b) slave, and (c) harvester.

The effect of the nonlinear stiffness coefficients of the master system $\alpha_1 = k_2 h^2 / k_1$ on the whole system dynamics is explored through Figure (6), where the system response curves at $\alpha_1 = -0.12, 0.2,$ and 0.75 is depicted. It is clear from the figure that the positive values of α_1 bend the response curve to the right to act as the hard spring Duffing oscillator, while the negative values of α_1 bend the response curves to respond as a soft spring Duffing oscillator having multiple solutions. To validate the accuracy of the plotted response curves in Figure (6), the whole system response curve is plotted again as in Figure (7) when $\alpha_1 = -0.12$ against the numerical solution of Equation (2), where the numerical solution is distinguished as small circles. It is obvious that the analytical solution and the result have excellent concordance. given by Equations (16) and the numerical solution obtained by applying the ODE45 algorithm. It is clear from Figure (7) also that the master-slave-harvester system may oscillate with a nonperiodic motion at $-0.5 < \sigma_1 < -0.21$.

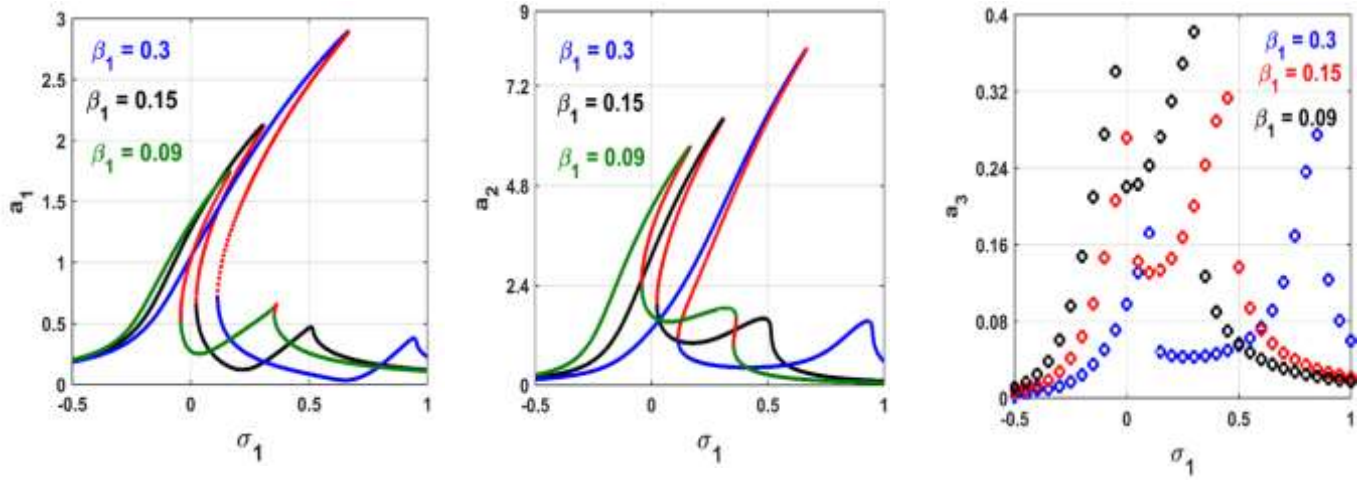

(a) (b) (c)

Figure 5. Oscillation amplitudes of the master-slave-harvester system at three different values of $\beta_1 = 0.09, 0.15,$ and 0.3: (a) master, (b) slave, and (c) harvester.

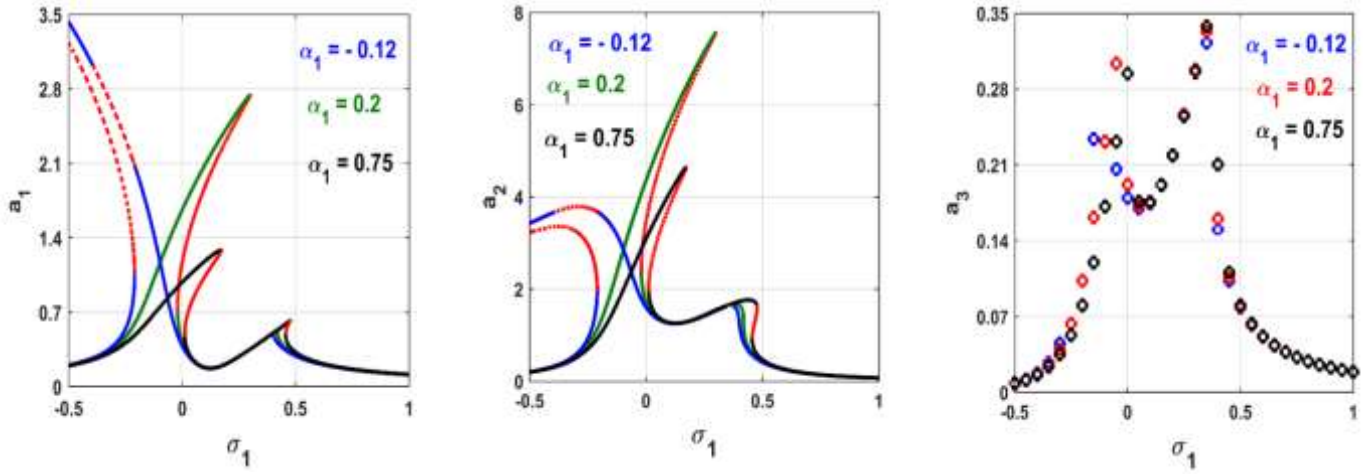

(a) (b) (c)

Figure 6. Oscillation amplitudes of the master-slave-harvester system at three different values of $\alpha_1 = -0.12, 0.2,$ and 0.75: (a) master, (b) slave, and (c) harvester.

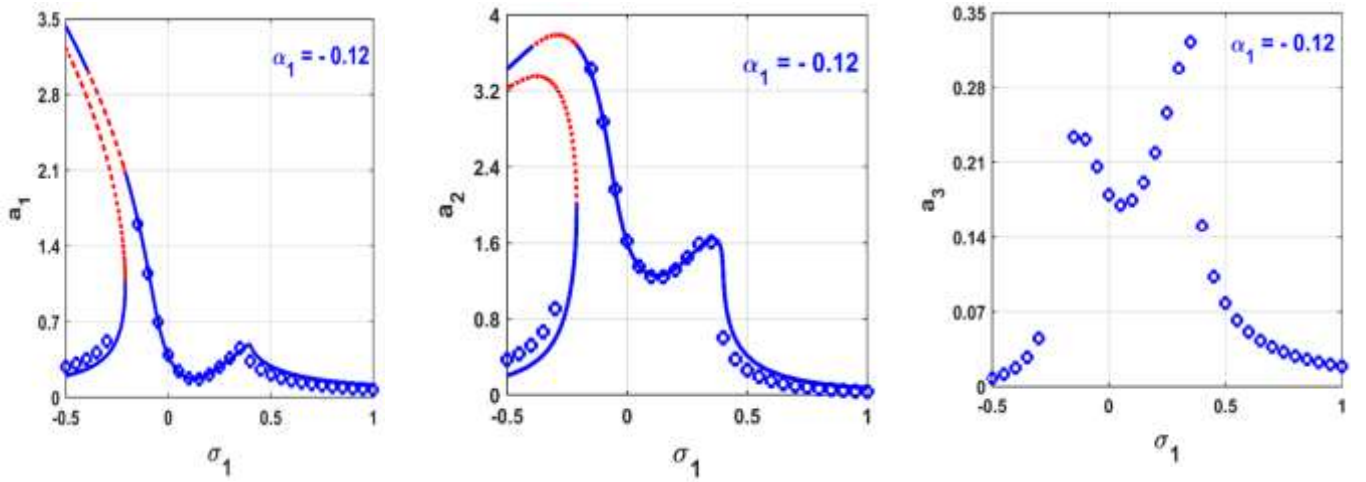

(a) (b) (c)

Figure 7. Oscillation amplitudes of the master-slave-harvester versus the numerical solution (small circle) according to Figure (6) when $\alpha_1 = -0.12$: (a) master, (b) slave, and (c) harvester.

The behavior of the proposed system for various absorber nonlinear stiffness coefficient values $\alpha_2 = k_4 h^2/k_1$ are investigated through Figures (8)-(10), where Figure (8) shows the system response curves at $\alpha_2 = -0.005, 0,$ and 0.008. The figure shows how the magnitudes of the nonlinear stiffness coefficient of the absorber have a significant impact on the dynamical behaviors of the entire system α_2, where the system may perform aperiodic motion on both sides of $\sigma_1 = 0$ according to the sign of α_2 either positive or negative.

In order to verify the response curves shown in Figure (8), The analytical solution is plotted against the numerical solution, represented by little circles given by Equation (16) when $\alpha_2 = 0.008$ as shown in Figures (9a), (9b), and (9c), where it is reported that the numerical and analytical studies are in excellent agreement. However, Figures (9a), (9b), and (9c) depicted that the master-slave system has three solutions when $\sigma_1 = 0.06$, in which two of these solutions are stable and one is unstable. The figures clearly show that of the two stable solutions, one has a high-oscillation amplitude and the other a small-oscillation amplitude, where the initial conditions determine whether the system under consideration will respond with a high or low oscillation. Finally, the instantaneous oscillations of the considered system according to Figure (9) when $\sigma_1 = 0.06$ at two initial sets (i.e., $x_1(0) = \dot{x_1}(0) = x_2(0) = \dot{x_2}(0) = x_3(0) = 0$ and $x_1(0) = 1.8,\ \dot{x_1}(0) = x_2(0) = \dot{x_2}(0) = x_3(0) = 0$) are simulated in Figure (10) from the graphic, it is obvious that the system exhibits low oscillations at $x_1(0) = \dot{x_1}(0) = x_2(0) = \dot{x_2}(0) = x_3(0) = 0$, while at $x_1(0) = 1.8,\ \dot{x_1}(0) = x_2(0) = \dot{x_2}(0) = x_3(0) = 0$, the system produces strong vibrations and hence harvests high voltage. Hence, it is possible to increase the generated power by controlling the initial conditions for a high harvesting energy.

B. Comparison study

We compared the performance of our proposed system with existing methods based on several parameters:

1. Function: this metric describes how the system act.
2. System parameters: parameters that control the dynamical system behavior.
3. System components.

And the results are shown in table 1.

	Ref [24]	Proposed paper
System components	Main system and absorber (only amass damper system with linear stiffness)	Main system and absorber (with linear and nonlinear stiffness, piezoelectric and RC circuit)
Function	Acting only as a vibration control	Not only vibration control but also energy harvester
System parameters	Little parameters	Many parameters

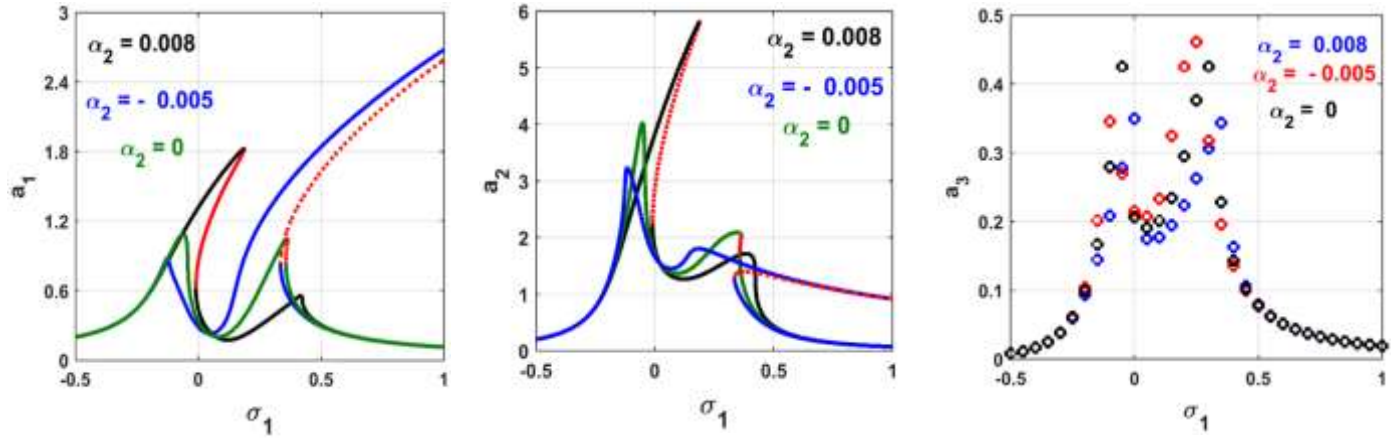

(a) (b) (c)

Figure 8. Oscillation amplitudes of the master-slave-harvester system at three different values of $\alpha_2 = -0.005, 0.0,$ and 0.008: (a) master, (b) slave, and (c) harvester.

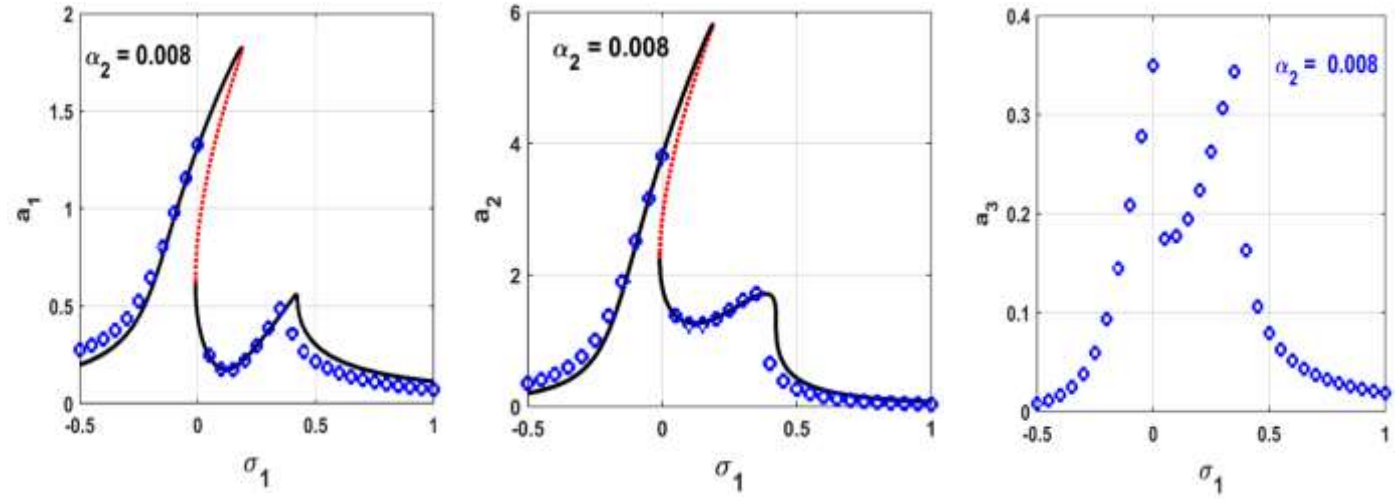

(a) (b) (c)

Figure 9. Oscillation amplitudes of the master-slave-harvester versus the numerical solution (small circle) according to Figure (9) when $\alpha_2 = 0.008$: (a) master, (b) slave, (c) harvester.

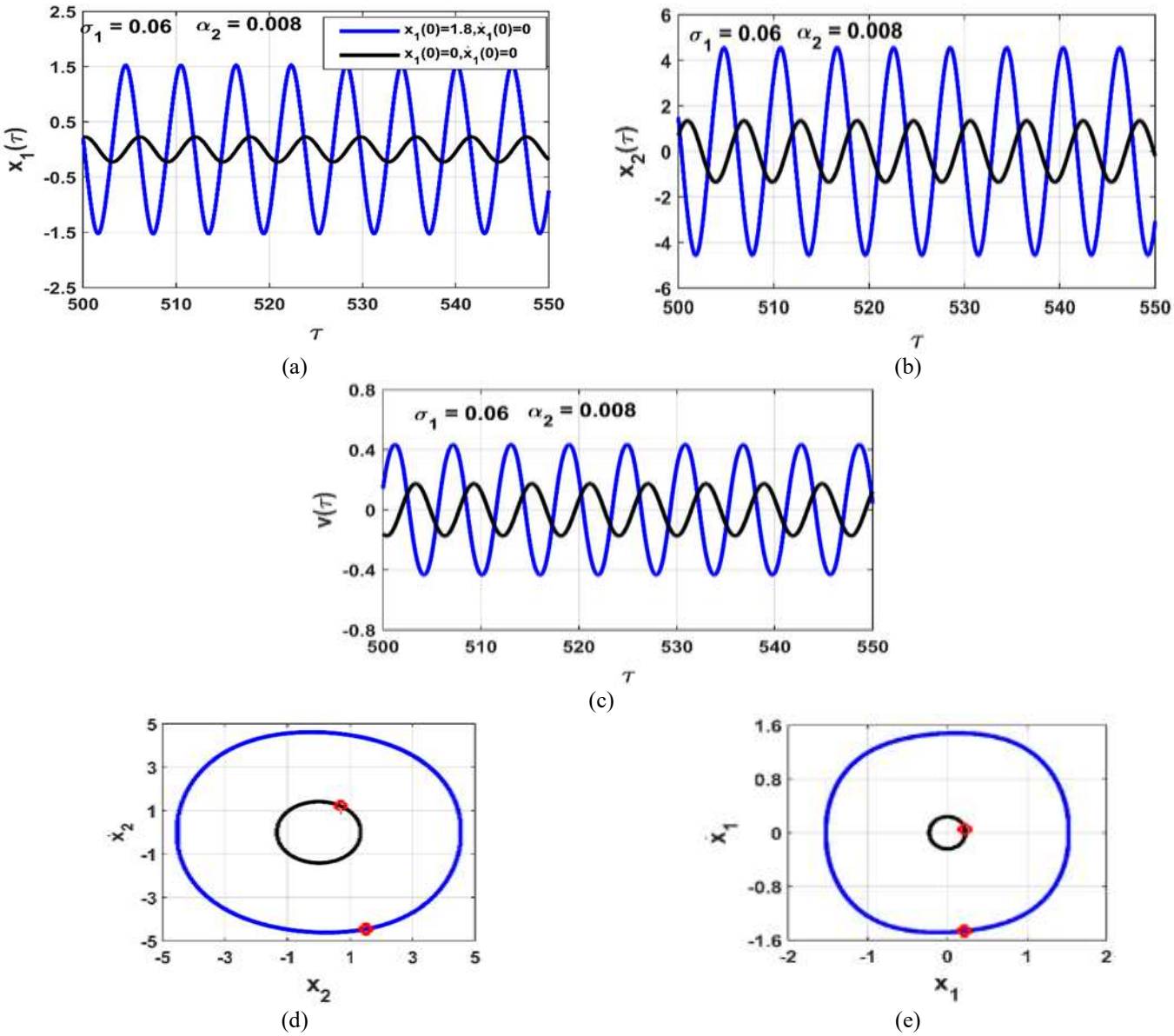

Figure 10. High and low harvesting voltage depending on the initial conditions according to Figure (10)) at $\sigma_1 = 0.06$: (a) master, (b) slave, (c) harvester, (d)master orbit plot and Poincare-map, (e) slave orbit plot and Poincare-map.

IV. CONCLUSIONS

The objective of this study is to examine the nonlinear dynamics of a master-slave system that is linked to a piezoelectric energy harvester. Perturbation methods are used to analyze the mathematical model of the whole system. The investigation concentrates on how different system parameters affect the vibration amplitudes and harvesting voltage. Through analytical results, the study identifies the ideal system parameters for both energy harvesting and vibration control objectives. In summary, this work presents optimal system parameters for energy harvesting and vibration control purposes, where the following concluded points can be summarized:

1. Depending on the desired goal, the slave system can be utilized as either a vibration absorber or an energy harvester by modifying the master-slave mass ratio in accordance with the excitation frequency.
2. Adjusting the master-slave linear stiffness ratio allows the slave system to operate as either a vibration absorber or an energy harvester depending on the excitation frequency, in line with its intended purpose.
3. Changing the nonlinear stiffness coefficient of either the master or slave system can cause instability throughout the system, leading to significant excitation amplitudes for energy harvesting, even with a small excitation force.
4. By taking advantage of the inherent nonlinearity of the system, it is possible to induce strong oscillation for energy harvesting purposes using only the initial conditions.

5. The conclusions drawn from this study emphasize the importance of modifying system parameters and initial conditions to achieve efficient energy harvesting and vibration control in the system under investigation.

Appendix

$$\frac{\partial F_1}{\partial a_{11}} = -\frac{1}{2}(\mu_1 + \beta_2) - \frac{1}{2}\frac{\eta\gamma_1\gamma_3}{(\omega_1^2+\eta^2)} - \frac{1}{\omega_1}(\frac{3}{2}\alpha_2 a_{10}a_{20})\sin(\varphi_{20}) + \frac{3}{4\omega_1}\alpha_2 a_{10}\ a_{20}\sin(\varphi_{20}) + \frac{3}{8\omega_1}\alpha_2 a_{20}^2\sin(2\varphi_{20}),$$

$$\frac{\partial F_1}{\partial a_{21}} = -\frac{1}{\omega_1}(\frac{1}{2}\beta_1 + \frac{9}{8}\alpha_2 a_{20}^2 + \frac{3}{4}\alpha_2 a_{10}^2 + \frac{1}{2}\frac{\omega_2^2\gamma_1\gamma_3}{(\omega_2^2+\eta^2)})\sin(\varphi_{20}) + \frac{1}{\omega_1}(\frac{1}{2}\omega_2\beta_2 + \frac{1}{2}\frac{\omega_2\gamma_1\gamma_3\eta}{(\omega_2^2+\eta^2)})\cos(\varphi_{20}) + \frac{3}{8\omega_1}\alpha_2 a_{10}^2\sin(\varphi_{20}) + \frac{3}{4\omega_1}\alpha_2 a_{10}\ a_{20}\sin(2\varphi_{20}),$$

$$\frac{\partial F_1}{\partial \varphi_{11}} = \frac{f}{2\omega_1}\cos(\varphi_{10}),$$

$$\frac{\partial F_1}{\partial \varphi_{21}} = -\frac{1}{\omega_1}(\frac{1}{2}\beta_1 a_{20} + \frac{3}{8}\alpha_2 a_{20}^3 + \frac{3}{4}\alpha_2 a_{10}^2 a_{20} + \frac{1}{2}\frac{\omega_2^2\gamma_1\gamma_3}{(\omega_2^2+\eta^2)}a_{20})\cos(\varphi_{20}) - \frac{1}{\omega_1}(\frac{1}{2}\omega_2\beta_2 a_{20} + \frac{1}{2}\frac{\omega_2\gamma_1\gamma_3\eta}{(\omega_2^2+\eta^2)}a_{20})\sin(\varphi_{20}) + \frac{3}{8\omega_1}\alpha_2 a_{10}^2\ a_{20}\cos(\varphi_{20}) + \frac{3}{4\omega_1}\alpha_2 a_{10}\ a_{20}^2\cos(2\varphi_{20}),$$

$$\frac{\partial F_2}{\partial a_{11}} = \frac{1}{\omega_2}(\frac{1}{2}\beta_3 + \frac{9}{8}\alpha_3 a_{10}^2 + \frac{3}{4}\alpha_3 a_{20}^2 + \frac{1}{2}\frac{\omega_1^2\gamma_2\gamma_3}{(\omega_1^2+\eta^2)})\sin(\varphi_{20}) + \frac{1}{\omega_2}(\frac{1}{2}\mu_2\omega_1 + \frac{1}{2}\frac{\eta\omega_1\gamma_2\gamma_3}{(\omega_1^2+\eta^2)})\cos(\varphi_{20}) - \frac{3}{8\omega_2}\alpha_3 a_{20}^2\sin(\varphi_{20}) - \frac{3}{4\omega_2}\alpha_3 a_{10}a_{20}\sin(2\varphi_{20}),$$

$$\frac{\partial F_2}{\partial a_{21}} = -\frac{1}{2}\mu_2 - \frac{1}{2}\frac{\gamma_2\gamma_3\eta}{(\omega_2^2+\eta^2)} + \frac{3}{2}\frac{1}{\omega_2}\alpha_3 a_{10}a_{20}\sin(\varphi_{20}) - \frac{3}{4\omega_2}\alpha_3 a_{10}a_{20}\sin(\varphi_{20}) - \frac{3}{8\omega_2}\alpha_3 a_{10}^2\sin(2\varphi_{20}),$$

$$\frac{\partial F_2}{\partial \varphi_{11}} = 0,$$

$$\frac{\partial F_2}{\partial \varphi_{21}} = \frac{1}{\omega_2}(\frac{1}{2}\beta_3 a_{10} + \frac{3}{8}\alpha_3 a_{10}^3 + \frac{3}{4}\alpha_3 a_{10}a_{20}^2 + \frac{1}{2}\frac{\omega_1^2\gamma_2\gamma_3}{(\omega_1^2+\eta^2)}a_{10})\cos(\varphi_{20}) - \frac{1}{\omega_2}(\frac{1}{2}\mu_2\omega_1 a_{10} + \frac{1}{2}\frac{\eta\omega_1\gamma_2\gamma_3}{(\omega_1^2+\eta^2)}a_{10})\sin(\varphi_{20}) - \frac{3}{8\omega_2}\alpha_3 a_{10}a_{20}^2\cos(\varphi_{20}) - \frac{3}{4\omega_2}\alpha_3 a_{10}^2 a_{20}\cos(2\varphi_{20}),$$

$$\frac{\partial F_3}{\partial a_{11}} = -\frac{3}{4\omega_1}\alpha_1 a_{10} - \frac{3}{4\omega_1}\alpha_2 a_{10} - \frac{1}{\omega_1 a_{10}^2}(\frac{1}{2}\beta_1 a_{20} + \frac{3}{8}\alpha_2 a_{20}^3 + \frac{1}{2}\frac{\omega_2^2\gamma_1\gamma_3}{(\omega_2^2+\eta^2)}a_{20})\cos(\varphi_{20}) + \frac{3}{4}\frac{1}{\omega_1}\alpha_2 a_{20}\cos(\varphi_{20}) - \frac{1}{\omega_1 a_{10}^2}(\frac{1}{2}\omega_2\beta_2 a_{20} + \frac{1}{2}\frac{\omega_2\gamma_1\gamma_3\eta}{(\omega_2^2+\eta^2)}a_{20})\sin(\varphi_{20}) - \frac{f}{2\ \omega_1 a_{10}^2}\cos(\varphi_{10}) + \frac{3}{8\omega_1}\hat{\alpha}_2\ \ a_{20}\cos(\varphi_{20}),$$

$$\frac{\partial F_3}{\partial a_{21}} = -\frac{3}{2\omega_1}\alpha_2 a_{20} + \frac{1}{\omega_1 a_{10}}(\frac{1}{2}\beta_1 + \frac{9}{8}\alpha_2 a_{20}^2 + \frac{3}{4}\alpha_2 a_{10}^2 + \frac{1}{2}\frac{\omega_2^2\gamma_1\gamma_3}{(\omega_2^2+\eta^2)})\cos(\varphi_{20}) + \frac{1}{\omega_1 a_{10}}(\frac{1}{2}\omega_2\beta_2 + \frac{1}{2}\frac{\omega_2\gamma_1\gamma_3\eta}{(\omega_2^2+\eta^2)})\sin(\varphi_{20}) + \frac{3}{8\omega_1}\alpha_2 a_{10}\cos(\varphi_{20}) - \frac{3}{4\omega_1}\alpha_2 a_{20}\cos(2\varphi_{20}),$$

$$\frac{\partial F_3}{\partial \varphi_{11}} = -\frac{f}{2\omega_1 a_{10}}\sin(\varphi_{10}),$$

$$\frac{\partial F_3}{\partial \varphi_{21}} = -\frac{1}{\omega_1 a_{10}}(\frac{1}{2}\beta_1 a_{20} + \frac{3}{8}\alpha_2 a_{20}^3 + \frac{3}{4}\alpha_2 a_{10}^2 a_{20} + \frac{1}{2}\frac{\omega_2^2\gamma_1\gamma_3}{(\omega_2^2+\eta^2)}a_{20})\sin(\varphi_{20}) + \frac{1}{\omega_1 a_{10}}(\frac{1}{2}\omega_2\beta_2 a_{20} + \frac{1}{2}\frac{\omega_2\gamma_1\gamma_3\eta}{(\omega_2^2+\eta^2)}a_{20})\cos(\varphi_{20}) - \frac{3}{8\omega_1}\alpha_2 a_1 a_2\sin(\varphi_{20}) + \frac{3}{4\omega_1}\alpha_2 a_2^2\sin(2\varphi_{20}),$$

$$\frac{\partial F_4}{\partial a_{11}} = \frac{3}{4\omega_1}\alpha_1 a_{10} + \frac{3}{4\omega_1}\alpha_2 a_{10} + \frac{1}{\omega_1 a_{10}^2}(\frac{1}{2}\beta_1 a_{20} + \frac{3}{8}\alpha_2 a_{20}^3 + \frac{1}{2}\frac{\omega_2^2\gamma_1\gamma_3}{(\omega_2^2+\eta^2)}a_{20})\cos(\varphi_{20}) - \frac{3}{4}\frac{1}{\omega_1}\alpha_2 a_{20}\cos(\varphi_{20}) + \frac{1}{\omega_1 a_{10}^2}(\frac{1}{2}\omega_2\beta_2 a_{20} + \frac{1}{2}\frac{\omega_2\gamma_1\gamma_3\eta}{(\omega_2^2+\eta^2)}a_{20})\sin(\varphi_{20}) + \frac{f}{2\omega_1 a_{10}^2}\cos(\varphi_{10}) - \frac{3}{8\omega_1}\alpha_2 a_{20}\cos(\varphi_{20}) - \frac{3}{2\omega_2}\alpha_3 a_{10} + \frac{1}{\omega_2 a_2}(\frac{1}{2}\beta_3 + \frac{9}{8}\alpha_3 a_{10}^2 + \frac{3}{4}\alpha_3 a_{20}^2 + \frac{1}{2}\frac{\omega_1^2\gamma_2\gamma_3}{(\omega_1^2+\eta^2)})\cos(\varphi_{20}) - \frac{1}{\omega_2 a_2}(\frac{1}{2}\mu_2\omega_1 + \frac{1}{2}\frac{\eta\omega_1\gamma_2\gamma_3}{(\omega_1^2+\eta^2)})\sin(\varphi_{20}) + \frac{3}{8\omega_2}\alpha_3 a_{20}\cos(\varphi_{20}) - \frac{3}{4\omega_2}\alpha_3 a_{10}\cos(2\varphi_{20}),$$

$$\frac{\partial F_4}{\partial a_{21}} = \frac{3}{2\omega_1}\alpha_2 a_{20} - \frac{1}{\omega_1 a_{10}}(\frac{1}{2}\beta_1 + \frac{9}{8}\alpha_2 a_{20}^2 + \frac{3}{4}\alpha_2 a_{10}^2 + \frac{1}{2}\frac{\omega_2^2\gamma_1\gamma_3}{(\omega_2^2+\eta^2)})\cos(\varphi_{20}) - \frac{1}{\omega_1 a_{10}}(\frac{1}{2}\omega_2\beta_2 + \frac{1}{2}\frac{\omega_2\gamma_1\gamma_3\eta}{(\omega_2^2+\eta^2)})\sin(\varphi_{20}) - \frac{3}{8\omega_1}\alpha_2 a_{10}\cos(\varphi_{20}) + \frac{3}{4\omega_1}\alpha_2 a_{20}\cos(2\varphi_{20}) - \frac{3}{4\omega_2}\alpha_3 a_{20} - \frac{1}{\omega_2 a_{20}^2}(\frac{1}{2}\beta_3 a_{10} + \frac{3}{8}\alpha_3 a_{10}^3 + \frac{1}{2}\frac{\omega_1^2\gamma_2\gamma_3}{(\omega_1^2+\eta^2)}a_{10})\cos(\varphi_{20}) + \frac{3}{4}\frac{1}{\omega_2}\alpha_3 a_{10}\cos(\varphi_{20}) + \frac{1}{\omega_2 a_{20}^2}(\frac{1}{2}\mu_2\omega_1 a_{10} + \frac{1}{2}\frac{\eta\omega_1\gamma_2\gamma_3}{(\omega_1^2+\eta^2)}a_{10})\sin(\varphi_{20}) + \frac{3}{8\omega_2}\alpha_3 a_{10}\cos(\varphi_{20}),$$

$$\frac{\partial F_4}{\partial \varphi_{11}} = \frac{f}{2\omega_1 a_{10}}\sin(\varphi_{10}),$$

$$\frac{\partial F_4}{\partial \varphi_{21}} = \frac{1}{\omega_1 a_{10}}(\frac{1}{2}\beta_1 a_{20} + \frac{3}{8}\alpha_2 a_{20}^3 + \frac{3}{4}\alpha_2 a_{10}^2 a_{20} + \frac{1}{2}\frac{\omega_2^2\gamma_1\gamma_3}{(\omega_2^2+\eta^2)}a_{20})\sin(\varphi_{20}) - \frac{1}{\omega_1 a_{10}}(\frac{1}{2}\omega_2\beta_2 a_{20} + \frac{1}{2}\frac{\omega_2\gamma_1\gamma_3\eta}{(\omega_2^2+\eta^2)}a_{20})\cos(\varphi_{20}) + \frac{3}{8\omega_1}\alpha_2 a_{10}\ a_{20}\sin(\varphi_{20}) - \frac{3}{4\omega_1}\alpha_2 a_{20}^2\sin(2\varphi_{20}) - \frac{1}{\omega_2 a_{20}}(\frac{1}{2}\beta_3 a_{10} + \frac{3}{8}\alpha_3 a_{10}^3 + \frac{3}{4}\alpha_3 a_{10} a_{20}^2 + \frac{1}{2}\frac{\omega_1^2\gamma_2\gamma_3}{(\omega_1^2+\eta^2)}a_{10})\sin(\varphi_{20}) - \frac{1}{\omega_2 a_{20}}(\frac{1}{2}\mu_2\omega_1 a_{10} + \frac{1}{2}\frac{\eta\omega_1\gamma_2\gamma_3}{(\omega_1^2+\eta^2)}a_{10})\cos(\varphi_{20}) - \frac{3}{8\omega_2}\alpha_3 a_{10} a_{20}\sin(\varphi_{20}) + \frac{3}{4\omega_2}\alpha_3 a_1^2\sin(2\varphi_{20}).$$

Compliance with Ethical Standards

Acknowledgments:

- This work has been supported by the Polish National Science Centre, Poland under the grant OPUS 18 No. 2019/35/B/ST8/00980.

Declaration of Conflicting Interests:

- The authors declare no potential conflicts of interest concerning the research, authorship, and/or publication of this article.

V.

EFERENCES

[1] J. Hunt, "Dynamic Vibration Absorbers," Journal of Sound and Vibration, vol. 78, no. 4, p. 609, 1980.

[2] Y. Du, R. A. Burdisso and E. Nikolaidis, "Control of internal resonances in vibration isolators using passive and hybrid dynamic vibration absorbers," Journal of Sound and Vibration, vol. 286, no. 4-5, pp. 697-727, 2005.

[3] Y. Cheung and W. Wong, "H∞ and H2 optimizations of a dynamic vibration absorber for suppressing vibrations in plates," Journal of Sound and Vibration, vol. 320, no. 12, pp. 29-42, 2009.

[4] J. Hunt and J.-C. Nissen, "The broadband dynamic vibration absorber," Journal of Sound and Vibration, vol. 83, no. 4, pp. 573-578, 1982.

[5] C. W. BERT, D. M. EGLE, WILKINS and D. J. JR, "Optimal design of a non-linear dynamic absorber," Journal of sound and vibration., vol. 137, no. 2, pp. 347-352, 1990.

[6] S. Natsiavas, "Steady state oscillations and stability of non-linear dynamic vibration absorbers," Journal of Sound and Vibration, vol. 156, no. 2, pp. 227-245, 1992.

[7] Z. Yang, S. Zhou, J. Zu and D. Inman, "High-Performance Piezoelectric Energy Harvesters and Their Applications," joule, vol. 2, no. 4, pp. 642-697, 2018.

[8] N. Stephen, "On energy harvesting from ambient vibration," Journal of Sound and Vibration, vol. 293, no. 1-2, pp. 409-425, 2006.

[9] N. E. duToit and B. L. Wardle, "Experimental Verification of Models for Microfabricated Piezoelectric Vibration Energy Harvesters," AIAA J, vol. 45, no. 5, 2007.

[10] K. Vijayan, M. I. Friswell, H. H. Khodaparast and S. Adhikari, "Energy Harvesting in a Coupled System Using Nonlinear Impact," Structural Health Monitoring, vol. 5, p. 255–261, 2014.

[11] D. D. Quinn, A. L. Triplett, A. F. Vakakis and L. A. Bergman, "Energy Harvesting From Impulsive Loads Using Intentional Essential Nonlinearities," vol. 133, no. 1, 2011.

[12] M. Belhaq and M. Hamdi, "Energy harvesting from quasi-periodic vibrations," Nonlinear Dynamics, vol. 86, p. 2193–2205, 2016.

[13] Saeed, N.A.; Mahrous, E.; Awrejcewicz, J. Nonlinear dynamics of the six-pole rotor-AMB system under two different control configurations. Nonlinear Dyn 2020, 101, 2299–2323.

[14] Saeed, N. A.; Awwad, E. M.; El-Meligy, M. A.; Nasr, E. S. A. Radial versus cartesian control strategies to stabilize the non-linear whirling motion of the six-pole rotor-AMBs. IEEE Access 2020, 8, 138859-138883.

[15] Saeed, N.A.; Mahrous, E.; Abouel Nasr, E.; Awrejcewicz, J. Nonlinear Dynamics and Motion Bifurcations of the Rotor Active Magnetic Bearings System with a New Control Scheme and Rub-Impact Force. Symmetry 2021, 13, 1502.

[16] El-Shourbagy, S. M.; Saeed, N.A.; Kamel, M.; Raslan, K.R.; Aboudaif, M.K.; Awrejcewicz, J. Control Performance, Stability Conditions, and Bifurcation Analysis of the Twelve-Pole Active Magnetic Bearings System. Appl. Sci. 2021, 11, 10839.

[17] Saeed, N.A.; Awwad, E.M.; El-Meligy, M.A.; Nasr, E.S.A. Analysis of the rub-impact forces between a controlled nonlinear rotating shaft system and the electromagnet pole legs. Applied Mathematical Modelling 2021, 93, 792-810.

[18] L. Tang and Y. Yang, "A multiple-degree-of-freedom piezoelectric energy harvesting model," Journal of Intelligent Material Systems, vol. 23, no. 14, p. 1631–1647, 2012.

[19] H. Wang, A. Jasim and X. Chen, "Energy harvesting technologies in roadway and bridge for different applications – A comprehensive review," Applied Energy, vol. 212, pp. 1083-1094, 2018.

[20] X. Tang and L. Zuo, "Vibration energy harvesting from random force and motion excitations," Smart Materials and Structures, vol. 21, no. 7, 2012.

[21] Y. Zhang, L. Tang and K. Liu1, "Piezoelectric energy harvesting with anonlinear energy sink," Journal of Intelligent Material Systems and Structures, vol. 28, no. 3, p. 307–322, 2017.

[22] X. Li, Y.-W. Zhang, H. Ding and L.-Q. Chen, "Dynamics and evaluation of anonlinear energy sink integrated by a piezoelectric energy harvester under a harmonic excitation," Journal of Vibration and Control, vol. 25, no. 4, p. 851–86, 2019.

[23] J. H. Bonsel, R. H. B. Fey and H. Nijmeijer, "Application of a Dynamic Vibration Absorber to a Piecewise Linear Beam System," Nonlinear Dynamics, vol. 37, p. 227–243, 2004.

[24] J. Ji and N. Zhang, "Suppression of the primary resonance vibrations of a forced nonlinear system using a dynamic vibration absorber," Journal of Sound and Vibration, vol. 329, no. 11, pp. 2044-2056, 2010.

[25] M. Karama, M. Hamdi and M. Habbad, "Energy harvesting in a nonlinear energy sink absorber using delayed resonators," Nonlinear Dynamics, vol. 105, p. 113–129, 2021.

[26] Nayfeh, A. H.; Mook, D.T. Non-linear Oscillations; Wiley: New York, NY, USA, 1995.

[27] Nayfeh, A.H. Resolving Controversies in the Application of the Method of Multiple Scales and the Generalized Method of Averaging. Non-linear Dyn 2005, 40, 61–102.

[28] Slotine, J.-J.E.; Li, W. Applied Non-linear Control. Prentice Hall, Englewood Cliffs, 1991.